COMBINING QUALITY, PERFORMANCE & EFFICIENCY IN CFD PRE-PROCESSING

Evangelos Skaperdas*, Christos Kolovos
BETA CAE Systems S.A., Greece

KEYWORDS - CFD pre-processing, CFD best-practices, meshing, model organization, morphing

ABSTRACT - The creation of mesh models for complicated automotive applications is an increasing challenge as demands for high simulation accuracy and short time cycles are mandated by current market needs. Several steps are included in the preparation of a CFD model and some of them are quite laborious. Many advances have taken place in fully automatic pre-processing for structural applications, but the additional complexity of CFD pre-processing does not allow this yet. The best possible solution for CFD pre-processing must balance well between mesh quality, which will allow and ensure reliable simulation results, and process efficiency with respect to time of manual and automatic operations and the handling of very large amounts of data.

Accepting the fact that user intervention and actions are currently required to ensure a high quality mesh, a case study of a CFD model creation for a racing motorbike is here presented. Following all common CFD recommended practices, a complete mesh model is prepared in ANSA. An investigation of the feasibility of the generation of various mesh configurations and densities with respect to user effort is made. In particular, the geometrical complexity of the model with its multiple interconnected zero-thickness walls provides a challenge for the generation of boundary layer volume elements. In addition, the treatment of the exposed sides of the boundary layer elements with and without conformal interfaces is considered. Representative simulation results are presented and compared to available literature findings. Finally, mesh morphing is performed to examine the possibilities of reshaping and reusing the same mesh model to modify the motorbike's flow characteristics.

TECHNICAL PAPER -

1. CURRENT STATUS AND OBSTACLES IN CFD PRE-PROCESSING

The preparation of a mesh for CFD analysis of an automotive application is a complex and laborious process that used to require large amounts of man hours from experienced users and usually involved the combination of different software that are designed for specific tasks. All this, in combination with the huge model sizes that are currently necessary for realistic and accurate CFD simulations and are nowadays feasible by the available hardware resources, make the process stiff and error prone. Many advances have taken place in fully automatic pre-processing for structural applications, but the additional complexity of CFD pre-processing (mainly watertight preparation and dependency of volume mesh on surface mesh) does not allow this yet. The process usually consists of the steps shown in Table 1.
Several of these steps are currently straight forward within the ANSA pre-processing environment, like for example the input of CAD data. The available CAD translators (for Catia v4 and v5, Unigraphics, ProEngineer and JT Open) offer automated and error free geometry input and diminish the need for cleanup operations. Even with traditional neutral CAD data exchange formats (IGES, STEP etc.) the powerful geometry handling capabilities of ANSA make cleanup a simple task.

Geometry Handling	- CAD data input - Cleanup - Outer surface extraction - Watertight creation - De-featuring - Treatment of proximities - Computational domain and sub-volume definitions
Meshing	- Surface meshing - Boundary layer elements generation - Volume meshing
Model Organization	- PDM and CFD solver specific Part Name Conventions - Boundary condition specification - Model integrity checks

Table 1: Typical steps involved in the pre-processing of a CFD model

The more complicated task of outer surface extraction is a step that can vary in difficulty depending on the data and communication with the CAD department. Standard conventions, like for example the management of Parts in different CAD layers for different use, that can be established in cooperation between the CAD and CAE people, can ensure that the CAE side gets only the information that is necessary. Still, ANSA possesses the tools that are needed for the extraction of outer flow-wetted surfaces, from thin sheet parts, as well as thick assemblies, as shown in Figure 1.

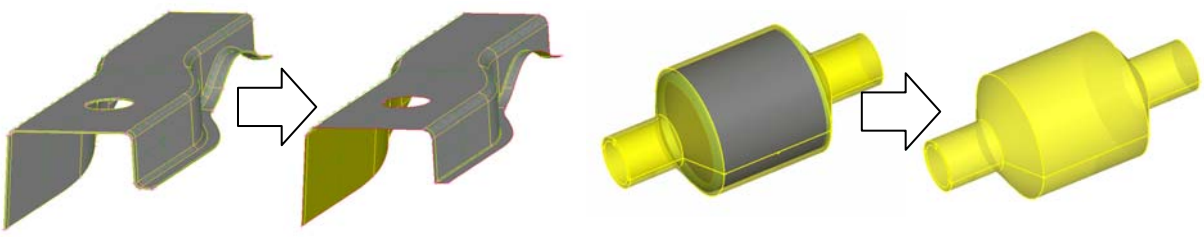

Figure 1: Extraction of outer surface examples in thin parts and thick assemblies

The creation of a watertight-model, that is a model that is fully closed for valid volume definitions, is currently the most difficult obstacle. There are many areas where sheet metal parts overlap and these need to be merged together into a single outer surface. Also there are several gaps that need to be sealed (Figure 2). Although development in the automation of these tasks is underway, for the moment this is a manual operation.

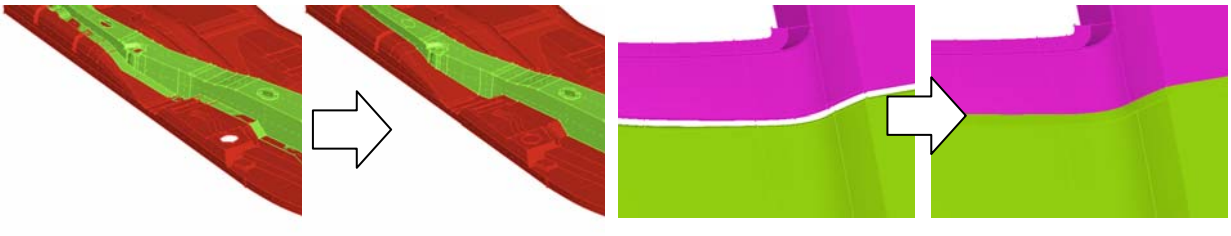

Figure 2: Generation of a watertight model: examples of overlapping flanges and gap closures

The de-featuring step (removal of small, unimportant for the flow simulation, features) is also something that can be handled easily in ANSA both in geometry and in mesh level. In the first case, the user can modify the geometry locally using the available CAD tools, while in the second the user can join macros together so that the mesh will flow over them uninterrupted. The benefit of the latter approach is that the original geometry remains unaffected and all the de-featuring can be easily undone, if so required.

In the meshing step, a mesh of variable size is usually required, fine enough in certain areas while coarser in others, so as to capture all important flow features while remain within a reasonable range of element count, which can be handled by the available hardware and time resources.

Finally, all the model preparation must be implemented with the following issue in mind. The user must be able to manage the Part information extracted from the PDM system of the company, so as to trace it back if a modification is required, but they must also account for different name conventions which are required for the CFD solver needs. A double parallel Part reference system which can combine both can be very useful.

2. QUALITY, EFFICIENCY AND PERFORMANCE IN CFD PRE-PROCESSING

Model Quality is very important as it ensures that our CFD simulation will converge easily and that our results can be trustworthy. In addition quality, not only restricted in simple terms of element quality criteria, but also as the fidelity by which we discretize the model, ensures that we are, in fact, simulating the real problem and not one that has unintentionally lost its geometrical characteristics. Quality requires user control for the geometry handling and mesh resolution for different areas and specific case. Quality also requires consistency and this is something that may not be available among different users.

Efficiency, on the other hand, is demanded by the industry which is forced to compress the time cycles of CAE studies. Therefore quality cannot come at any cost.
To achieve Efficiency the process must rely as less as possible to user interaction and leave all the tedious and heavy workload to computers. Efficiency also implies the ability that once a model is completed, a modification can be implemented without having to restart the whole process loop from the beginning. Finally, an efficient process is one that is straight forward and achieved with few resources. Exchanging data between different software to perform specific steps for which each may be specialized adds in investment costs and in extra time and storage required for the data exchange between them. Ideally one software should be able to perform all the pre-processing tasks.

Finally, Performance is also an important issue as it refers to the ability of the hardware and software to handle the huge model sizes that CFD has always required in the most demanding end of the CAE world. Although hardware performance is mounting rapidly, the burden is also spread to the software's ability to manage the data based on smart algorithms and efficient programming techniques.

Although some automated solutions are commercially available in the market, their disadvantages include lack of absolute user control when needed, mesh quality issues that may have adverse effects in solver accuracy [1], and difficulty for the user to pin point the cause when the process fails for some reason. Finally, a lack of flexibility in the reusability of the model when certain modifications are required is also an issue with these approaches.

The best possible solution for CFD pre-processing must therefore balance between mesh quality that will allow and ensure reliable simulation results, and process efficiency with respect to time of manual and automatic operations and the handling of very large amounts of data. Accepting the fact that user intervention and actions are currently required to ensure a good quality mesh we will examine how we can facilitate and streamline the mesh model build up process by providing all the necessary tools for it.

In this study we will follow the ANSA approach, which combines Quality, Efficiency and Performance, and demonstrate that a high quality mesh, satisfying CFD best practices that will ensure an accurate and valid CFD simulation, can be created without great effort and user expertise.

3. TEST CASE STUDY: MODEL OF THE YAMAHA R1 MOTORCYCLE

The model of the YAMAHA R1 motorcycle was kindly provided by Advantage CFD for this study (Figure 4). The model was selected for the following reasons: it is characterized by several geometrical complexities, proximities and multiple inter-connected zero-thickness walls, which pose problems in the definitions of the volumes and also make the generation of boundary layers quite a difficult task. In addition, the model has relatively small dimensions, which means that for the same mesh resolutions used in typical current external aerodynamics simulations for cars, we end up with moderate mesh sizes with which we can ran simulations and derive conclusions very fast. Some basic dimensions of this model include a wheelbase of 1.42 m, and a frontal area of 0.645 m^2 and 0.493 m^2 with and without the rider respectively.

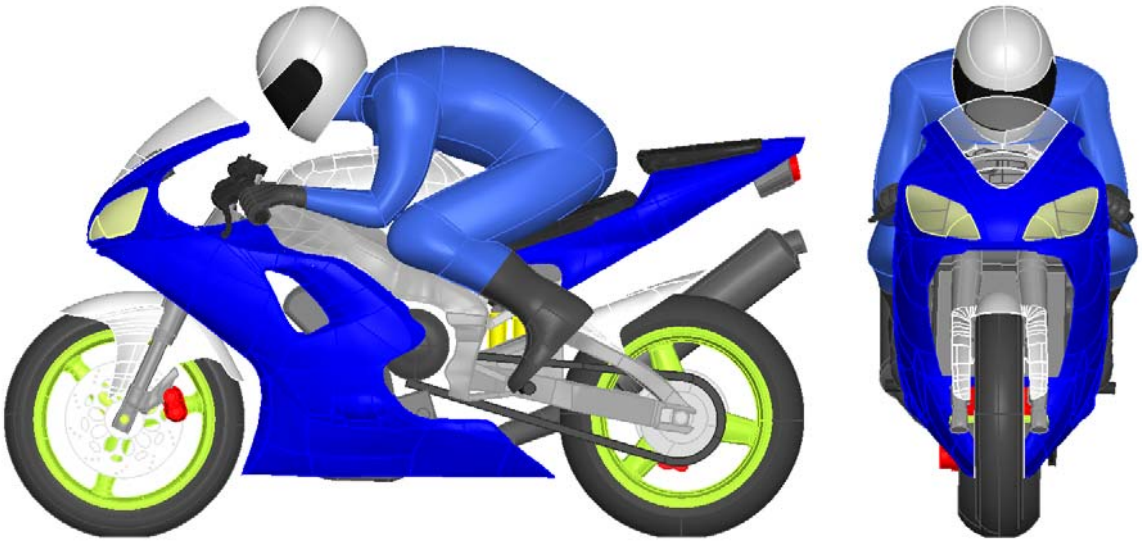

Figure 3: Geometry model of YAMAHA R1 (model courtesy of Advantage CFD)

Past work related to this was retrieved from the literature and includes the work of Piazza et al. [2] on a motorcycle without a rider, and Lewis et al. [3] on the same model. This current work focuses more on the mesh model preparation process and its impact on the simulation results, and goes a step beyond with respect to the generation of layers from all the complicated areas and the zero-thickness walls.
The commercial ANSA version 12.1.2 was used, with the exception of the generation of the layers from the zero-thickness walls, where the currently under development ANSA v12.2pre was used. All CFD simulations were performed with Fluent v6.3.26. The platforms involved were Windows XP Professional 64bit with P4 3.6GHz and XEON 2.66GHz processors and Linux Fedora Core 6 with AMD Athlon Dual Core 2.8GHz.

3.1 MODEL PREPARATION

The steps that were followed for the preparation of the CFD model are described bellow. The model was provided in ANSA database format so there were no translation or cleanup issues.

Computational Domain

A computational domain was constructed spanning 20 body lengths downstream, and 10 upstream as well as in the two lateral directions, as shown in Figure 4. This results in a very small blockage area ratio of 0.16 %, so the simulation refers to an open road test case.

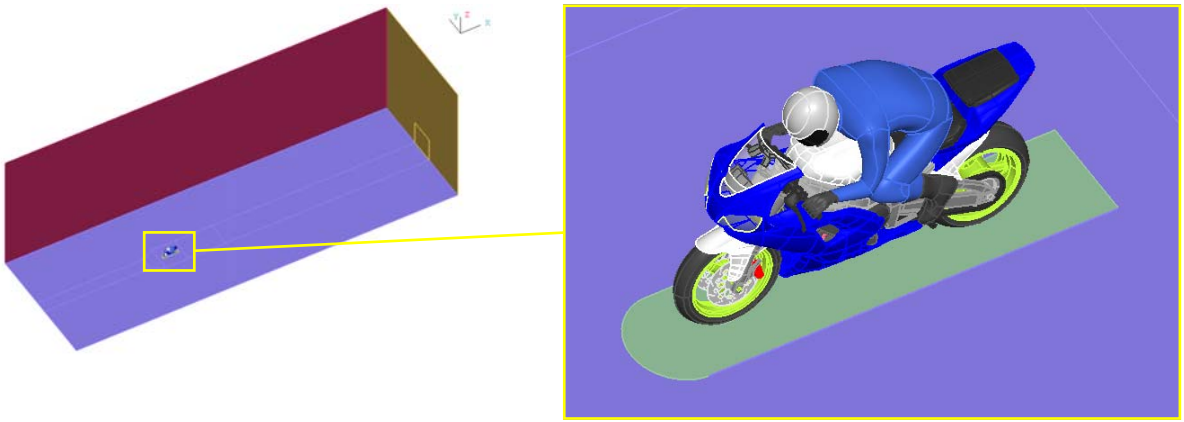

Figure 4: Computational domain and close up of motorcycle and rider model

Treatment Of Proximities In Geometry Level

Complicated automotive CFD models have several areas that suffer from narrow proximity problems. These usually result in bad tetra elements, or make the growth of layers impossible. The treatment of proximities in geometry level is something that can be treated efficiently in ANSA using the proximity detection algorithms and the "fuse" functionality. ANSA can isolate the Faces that are close together within a specified range and then, depending on the case, the user can employ the "fuse" function and either completely remove the enclosed space (Fig.5 left) or place it in a separate volume (Fig. 5 right) like for example the area around the wheel contact patch, which regardless if layers are grown or not, it is best to be volume-meshed separately. This allows the user to better prepare the surface mesh in that area.

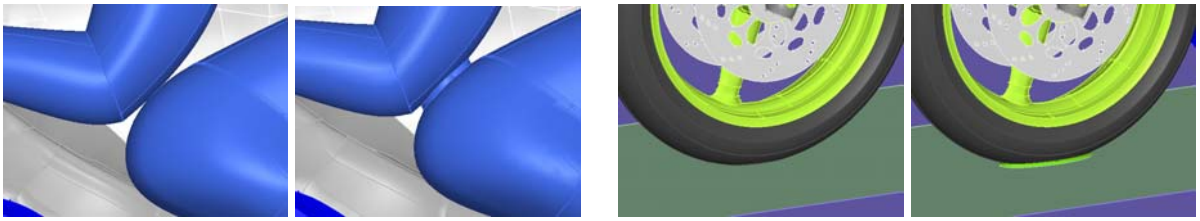

Figure 5: Treatment of proximities in geometry level using the "fuse" functionality

Definition Of Sub-Volumes And Management Of Parts And Properties

For the proper specification of the boundary conditions for the rotating wheels and the pressure drop of the radiator, separate sub volumes were constructed.
The creation of the Interior faces that enclose the sub-volumes inside the wheel and around the spokes area were carefully constructed to enclose only the proper volume, but also to avoid proximity with the disc brakes and to accommodate for the generation of the layers from both sides by being placed at a suitable normal angle from the wheel surfaces, as shown in Figure 6.

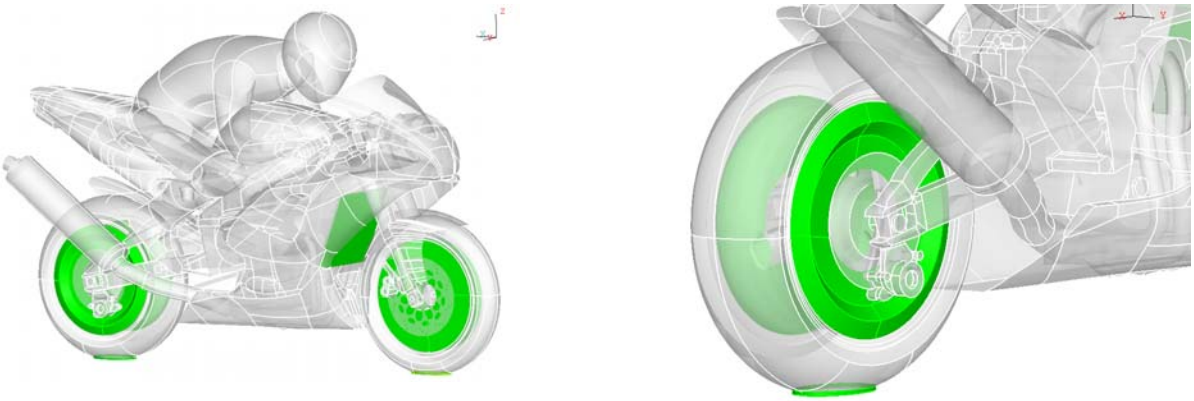

Figure 6: Definition of sub-volumes (shown in light green) for proper specification of boundary conditions in the solver.

To be able to handle this model, and other more complicated CFD models, the user must come up with a suitable part name convention, which will allow the simple management of the model for boundary condition specification in the solver as well as for post processing. Usually some parts are merged together so as to have fewer in the solver. However this leads to loss of Part reference information in the simulation,

The double and parallel Property (PID) and Part management system available in ANSA (Fig. 7) allows the user to keep the original Part Name, ID and hierarchy as extracted from the company's PDM system, while use a Part grouping and name convention suitable for the CFD solver, where for example they can give Properties name special prefixes so that they can quickly identify them within the solver environment. The ANSA Part Manager can also be used to manage the additional geometry that is created for the simulation, like the interior and computational domain boundary surfaces, as well as some points and curves that have information of the axes of rotation of the wheels for example.

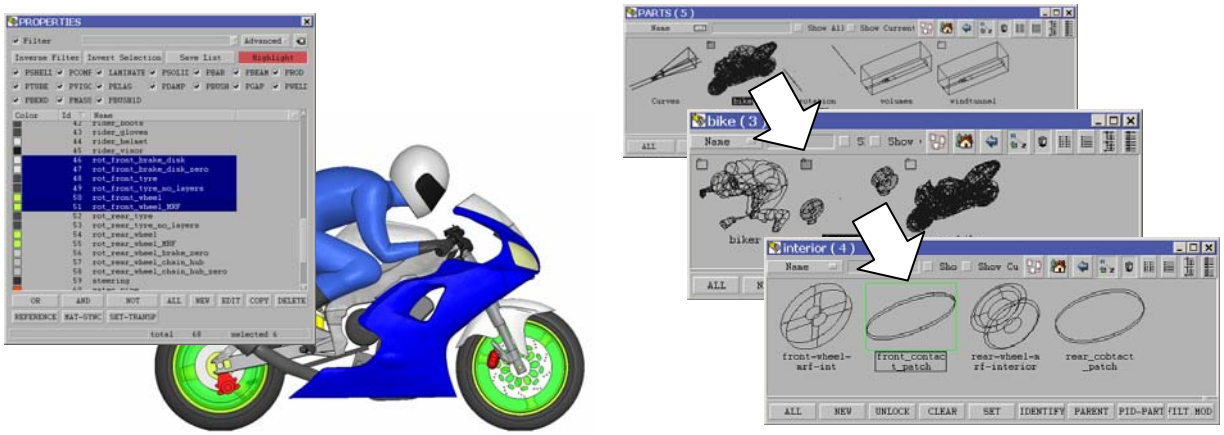

Figure 7: Model management through double name convention system: Property Names for CFD solver needs (left) and Part Manager (right).

Detection Of Zero Thickness Walls

The presence of zero-thickness walls in a model reduces the mesh size but adds complexity in the definition of boundary layers and volumes. The user cannot identify these parts by name, as there is no such information from CAD. In addition, the zero-thickness simplification may be done during the pre-processing step of geometry de-featuring, and some Parts may be half zero-thickness wall and half solid description. The identification of there areas and separation in different Property must be made.
The functionality of Volume Detection is ANSA is of great assistance in this case. The user can let ANSA detect all closed volumes in the model and then by removing these volumes from visible, only the zero thickness surfaces remain (see Fig. 8). These can be easily placed to separate PIDs with the same name plus a suffix like _zero_thickness. This will be very useful later when layers will be grown from these areas with the extra option to grow from both sides.

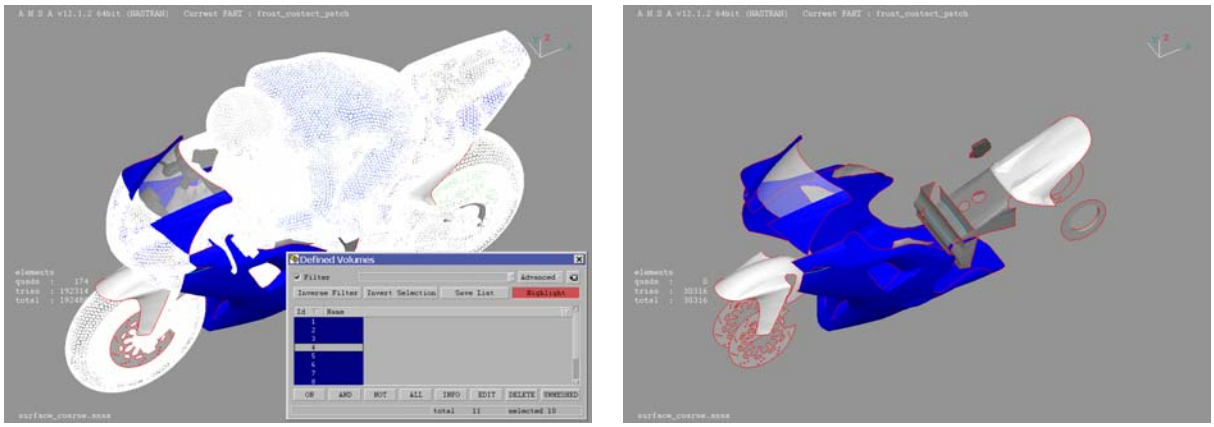

Figure 8: Detection and separation of zero-thickness wall surfaces for placement in separate PIDs

Assignment Of Boundary Condition Types

Having distributed and assigned the correct property names to all the parts, the user can also specify the boundary condition types for the Fluent solver (Fig. 9), so that the mesh can be read directly into the solver, with all the required information.

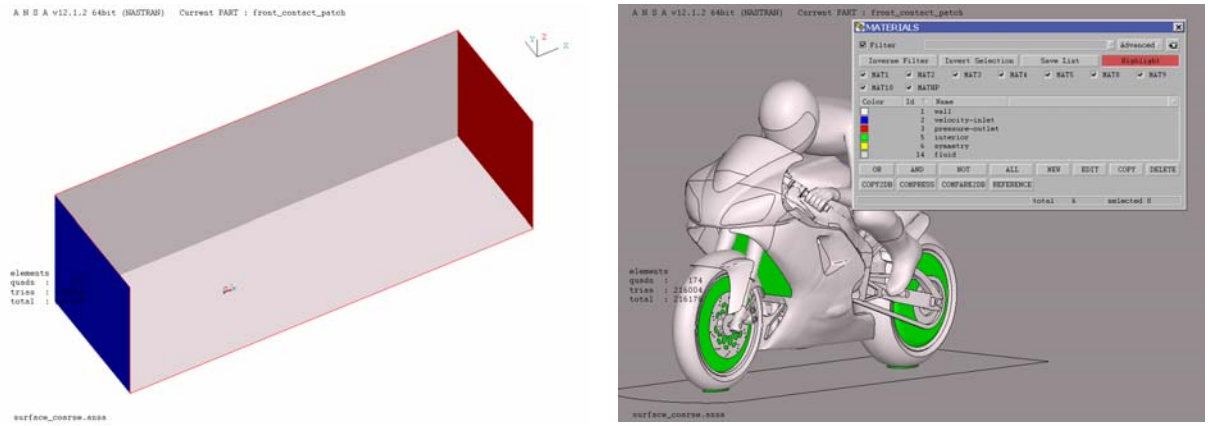

Figure 9: Definition of boundary condition types

Surface Meshing

The surface meshing step is very straight forward. Two surface meshes were generated. A coarse one, with more or less uniform element length, and a fine one, with size variation and refinement of all important areas.
The coarse mesh consists of 182 thousand surface elements (Fig. 10). It was prepared in around 15 min. This time also includes the fixing of some bad surfaces in the model and the quality improvement. Quality according to Fluent EquiArea skewness was kept below 0.5.

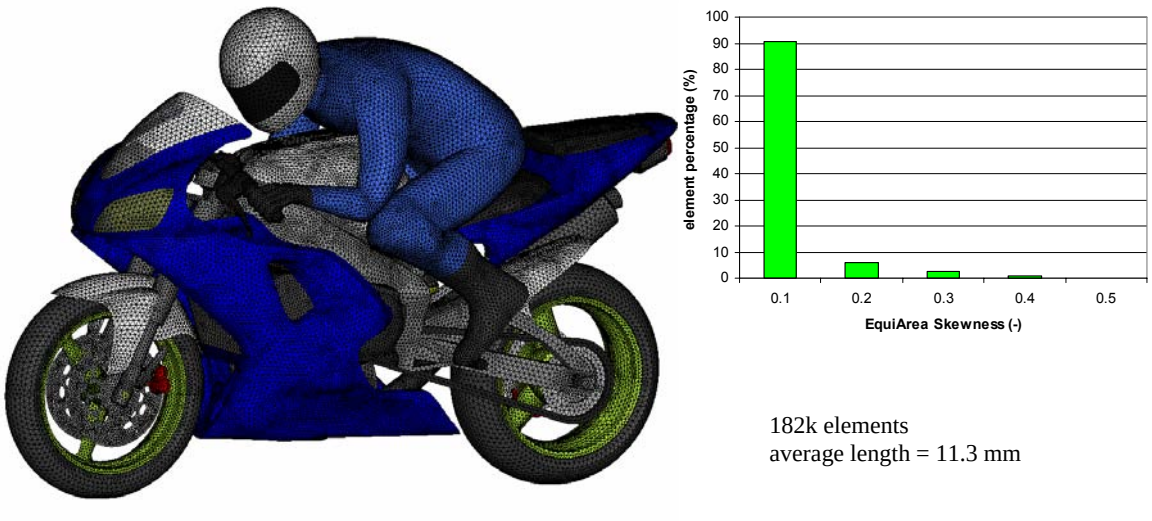

Figure 10: Coarse surface mesh

When a coarse mesh is used there may be some problems of proximity which were not considered initially at the geometry level, but arise now due to the large element length in these areas. ANSA functionality of proximity detection according to local element length and automatic refinement was employed to fix problems like the one shown in Figure 11.

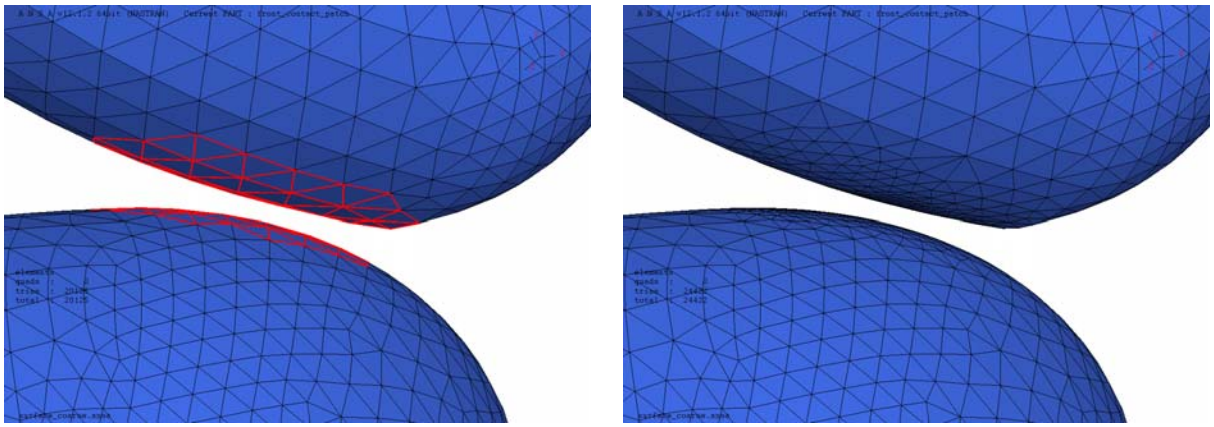

Figure 11: Treatment of proximities by automatic mesh refinement

The fine mesh consists of 544 thousand surface elements (Fig. 12). In this case the CFD spacing and meshing algorithm of ANSA was used. This allows the user to just specify a feature angle for the mesh, a growth rate, a minimum and a maximum length and ANSA meshes and refines automatically all the curvatures accordingly. In addition, the user can select to refine all sharp edges of the model where usually high gradients in the flow appear, down to a specific element length. Finally, using ANSA scripting all single and triple connectivity edges of the model, like the trailing edges of the zero-thickness walls were also automatically refined to a user specified value. This resulted in better mesh quality especially when the layers were grown, as the exposed quad facets at the free single boundaries were of good aspect ratio.

Mesh preparation and quality improvement was in this case even less than for the coarse mesh, as the smaller the minimum length, the fewer the elements and areas that needed improvement. With minimum manual work a high quality mesh was obtained. Fluent skewness was again below 0.5.

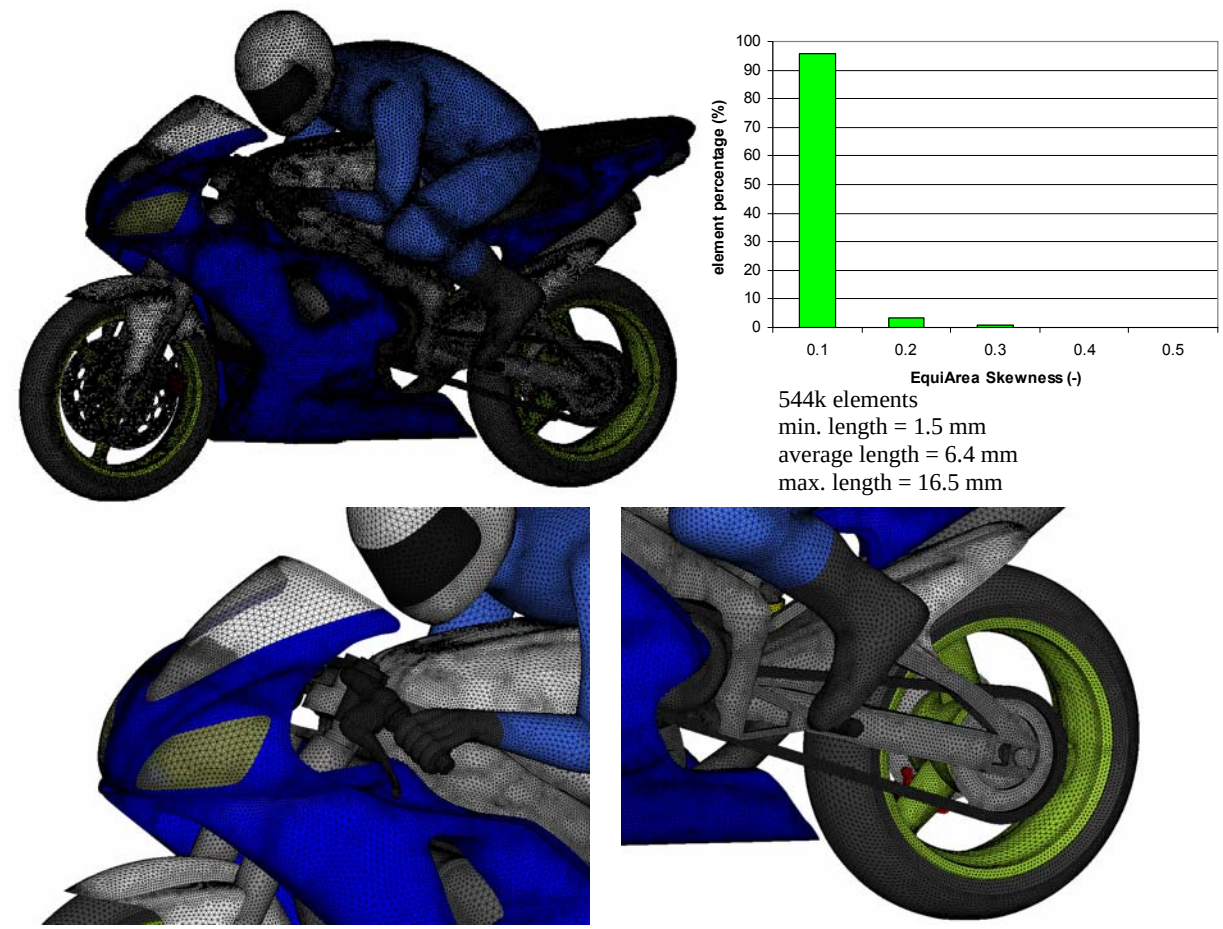

Figure 12: Fine surface mesh close ups

Meshing Of Small Sub Volumes

Having completed the surface mesh, the five sub-volumes that were constructed earlier (radiator, rotating volumes in wheels and volumes around contact patches) were meshed. The volumes around the contact patches were the ones with the worst elements, due to the very steep angle between the tyre and the road. Some manual fix was required there to ensure that Fluent EquiVolume skewness was kept below 0.95. The radiator was meshed with pentas.

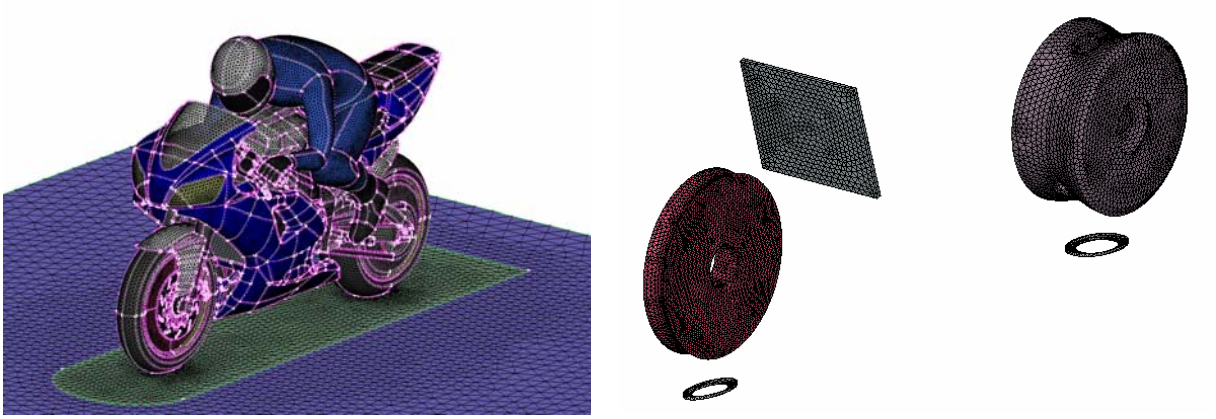

Figure 13: Volume meshing of small sub-volumes

Volume Meshing Of Main Domain

Based on the two surface meshes, three volume meshes (tetra coarse and fine and Hexa-Interior coarse) were created initially, without boundary layer elements, as shown in Figure 14. Time for volume meshing was between 5 to 15 minutes depending on the size of the mesh (from 3 to around 10 million elements). Refinement boxes were also placed to control the size of the elements around and downstream of the motorcycle.

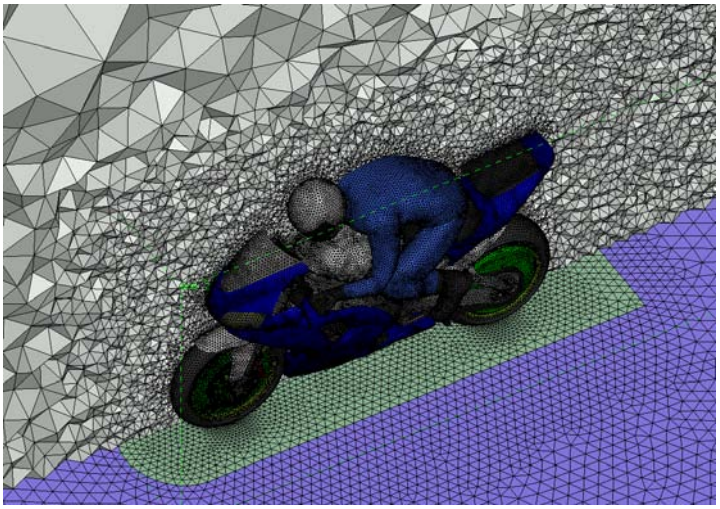

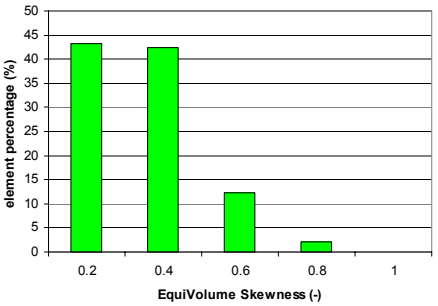

coarse tetra mesh 3.1 million
Refinement boxes:
Around bike max length = 50 mm
Along wake max length = 500 mm
Max tetra size = 1000 mm

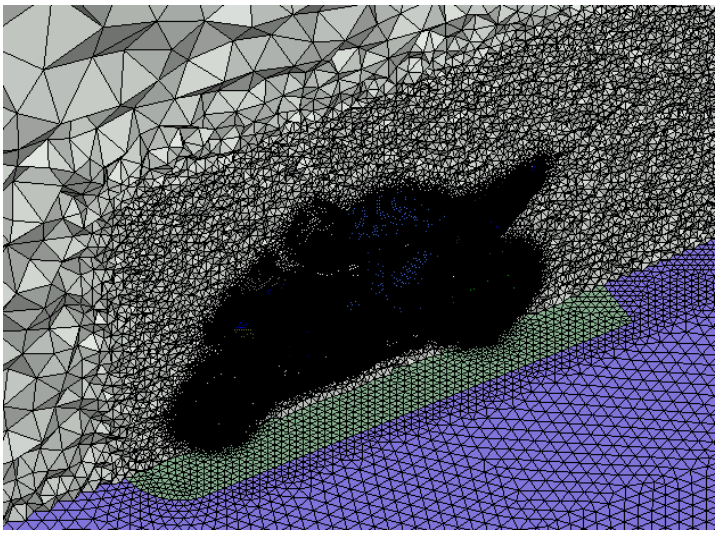

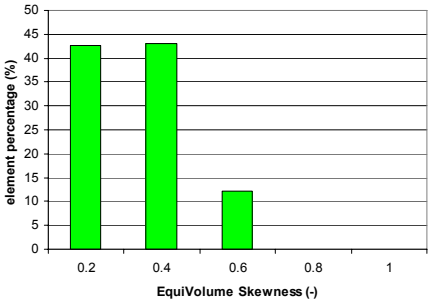

fine tetra mesh 9.8 million
Refinement boxes:
Around bike max length = 40 mm
Along wake max length = 250 mm
Max tetra size = 1000 mm

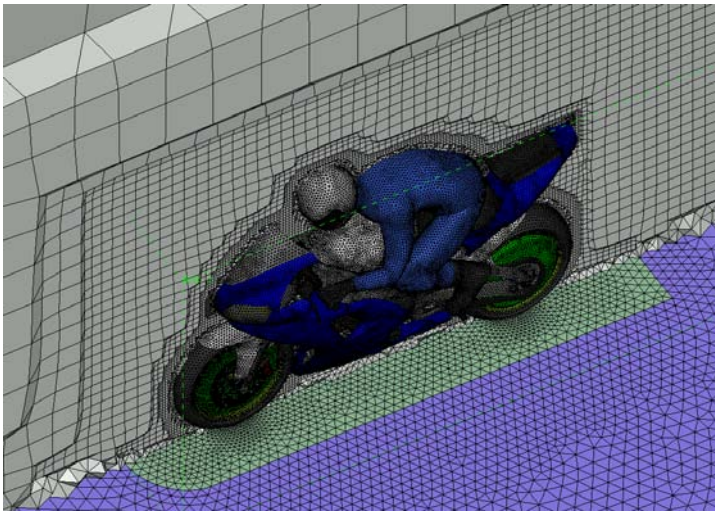

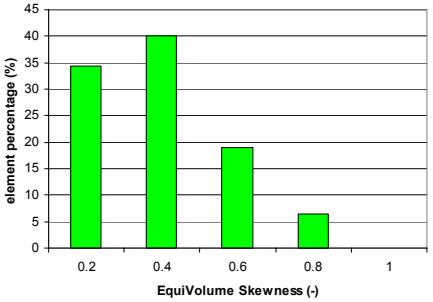

fine tetra mesh 3.2 million
Refinement boxes:
Around bike max length = 60 mm
Along wake max length = 500 mm
Max tetra size = 1000 mm

Figure 14: Volume meshes without layers

Volume Meshing With Boundary Layer Elements

To test the ability of ANSA v12.2pre under development version, boundary layer elements were generated from the coarse surface mesh. The advanced algorithm for the generation of layers lets the user to select the areas to grow layers from, with different parameters if required, and possesses clever algorithms that allow the automatic exclusion or certain areas that would result to the generation of bad quality elements or even intersections. Squeezing of layers is also available to avoid collisions and proximities. ANSA creates temporary shell elements in the excluded areas (shown in yellow in Fig 15) and thus does not modify the Properties of the original surface mesh. Five layers with growth rate 1.2 and first height 0.2 aspect were generated from all surfaces of the motorcycle and the rider. The layers were placed for demonstration purposes here in two different volume properties for the regular and the zero-thickness areas (red and purple respectively in Fig. 15).

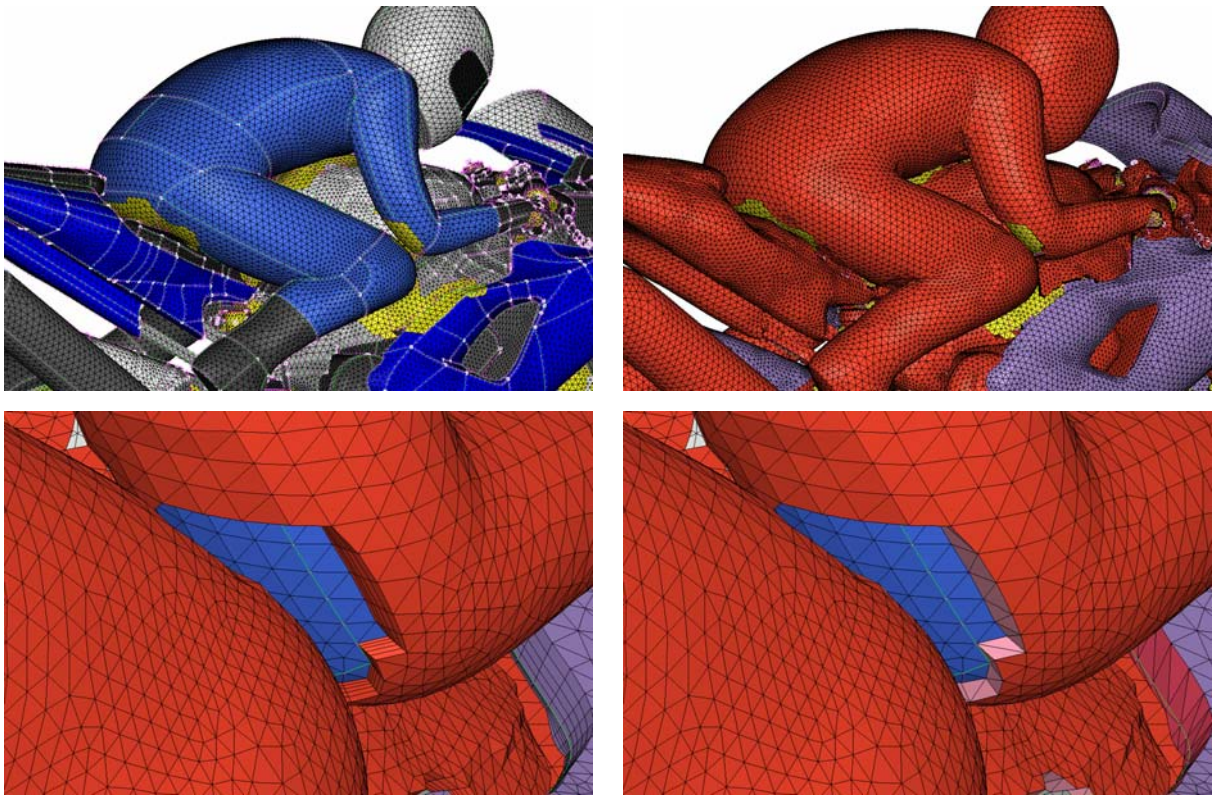

Figure 15: Generation of layers and excluded areas treatment

The exposed sides of the layers along the single boundaries or around the excluded areas are automatically treated in two ways: conformal quad facets or triangular non-conformal interfaces (Fig. 15). The definition of the outer remaining volume is a straight forward task as name conventions that are used to facilitate the isolation of the created shells that cover the layers. A volume mesh was then created consisting of 3.8 million elements (pentas and tetras). Note that for this model the layers were grown first from inside the rotating wheel sub-volumes and then from the outer main volume and were auto-connected to the interior boundary. Again for demonstration purposes the layers and the tetra mesh were placed in different properties, although for the actual simulation they were all merged in one.
Only the non-conformal approach was followed for the layer sides, as the generation of pyramids lead to bad elements. This subject is something that will be examined further to access the possibilities and the required development. Details of the model are shown in Figure 16.

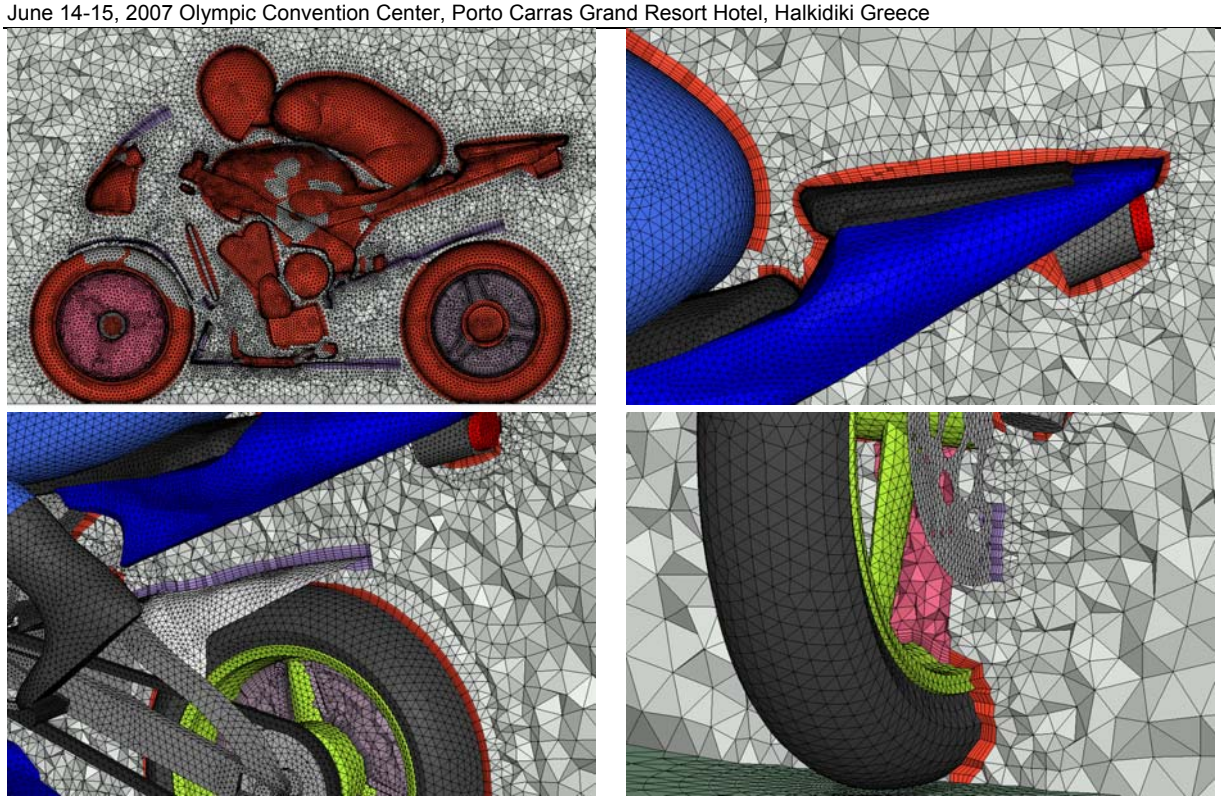

Figure 16: Details of the model with layers (3.8 million elements)

3.2 MORPHING THE COMPLETE MODEL

Having completed the models, the ANSA Morphing tool was used to make a modification of the front windscreen. The morphing boxes were constructed on the surface mesh model. The preparation time was less than 15 minutes. The boxes are snapped on the actual geometry of the model so that absolute control on all movements and deformations is available. The boxes extend outward by a considerable distance, thus allowing the mesh deformation to be distributed to more volume elements (Fig. 17). The morphing boxes were placed in a separate Part in the Part Manager so that they can be saved separately and later merged to the database with the complete volume mesh model, in this case the coarse tetra mesh model of 3.1 million elements. Then morphing is applied on both surface and volume.
The high quality of the volume mesh allowed the deformation of the front windscreen upwards by 70mm without deteriorating the mesh quality (skewness below 0.95). The morphing process is instantaneous and as many variants as required can be quickly output. The process can be also be parameterized and automated.

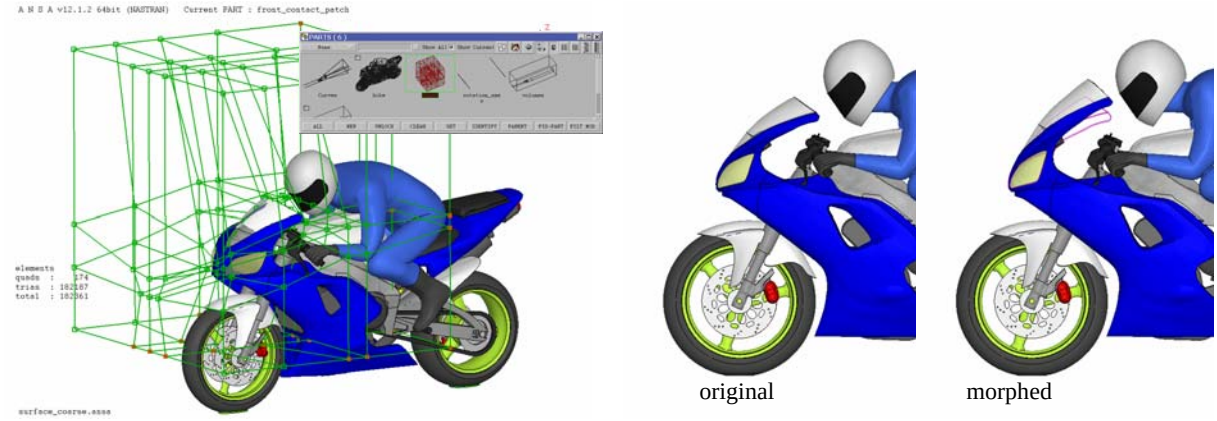

Figure 17: Morphing box setup and applied deformation of the front windscreen by 70 mm upwards.

3.3 SETUP OF THE CFD SIMULATION

The simulations were setup according to the best practices recommended by Fluent [4].
For simplification, steady state simulations were run. The k-ε realizable turbulence model was employed with non-equilibrium wall functions at the walls. A free stream velocity of 40 m/sec with 0.05% turbulence intensity and a turbulent viscosity ratio of 1 were applied. Translational velocity of 40 m/sec was also imposed on the road. The MRF model was used for the rotating wheel sub-volumes and rotational speeds for the wheels, tyres and disc brakes were applied. Symmetry conditions were used for the top and side boundaries. The porous model was used for the radiator with pressure drop calibration data from [5]. Fifty iterations were initially performed with first order discretization schemes for all variables and then 950 more with second order scheme.
Residuals and drag coefficient were monitored for all four cases. Figure 18 shows the smooth residual drop, indicating the quality of the model and the simulation setup.

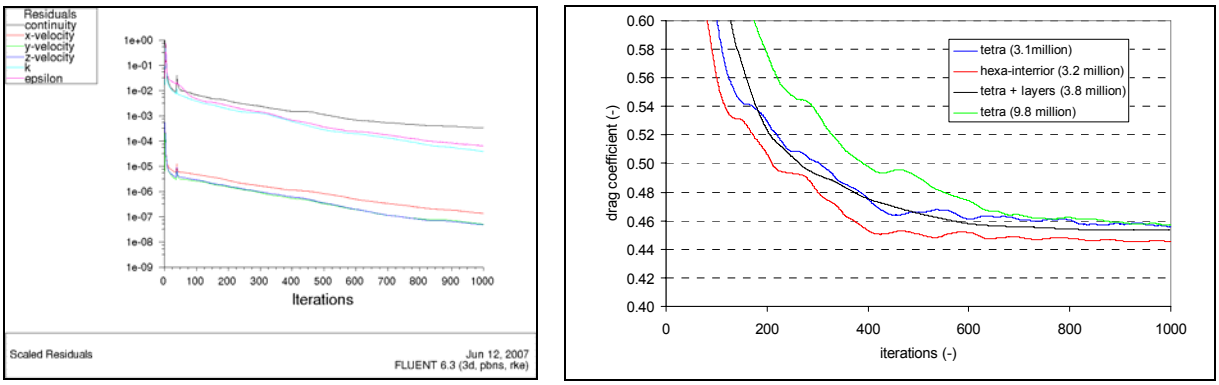

Figure 18: Representative residuals plots (for coarse tetra mesh case) and drag coefficient convergence history for the four different mesh configurations

3.4 COMPARISON OF RESULTS FROM DIFFERENT MESHES

Figure 18 shows that all four different mesh models converged to very similar drag coefficient predictions. Table 2 displays the drag coefficient and its two components, pressure and viscous drag, as well as the lift coefficient. The viscous contribution is around 5% of the total drag, which is expected as the rear wake of the model dominates. Lift is about 20% of the drag.

The two plain tetra meshes are in full agreement indicating mesh independent solution with respect to mesh refinement. The tetra plus layers and the hexa-interior meshes are also very close.

	C_D pressure	C_D viscous	C_D total	C_L total
tetra (3.1 million)	0.435	0.022	0.457	0.098
tetra (9.4 million)	0.434	0.024	0.458	0.105
tetra + layers (3.8 million)	0.430	0.023	0.453	0.093
hexa interior (3.2 million)	0.424	0.022	0.445	0.101

Table 2: Simulation results for four different meshes

Unfortunately, there are no experimental data for the exact motorcycle and the mesh models are not enough to draw exact conclusion as to which one is the most accurate, as some features that may gain in accuracy like the presence of layers and a fine mesh in the wake are not both present in one model.

Figure 19 shows velocity contours along the centre plane for the fine tetra and for the coarse tetra plus layers models. The fine tetra mesh has better refinement in the wake and shows better resolution of the flow in that area (especially close to the road), while the coarse tetra mesh with layers shows some low velocity areas downstream of the helmet and the rider's back which are not shown in the plain tetra mesh.

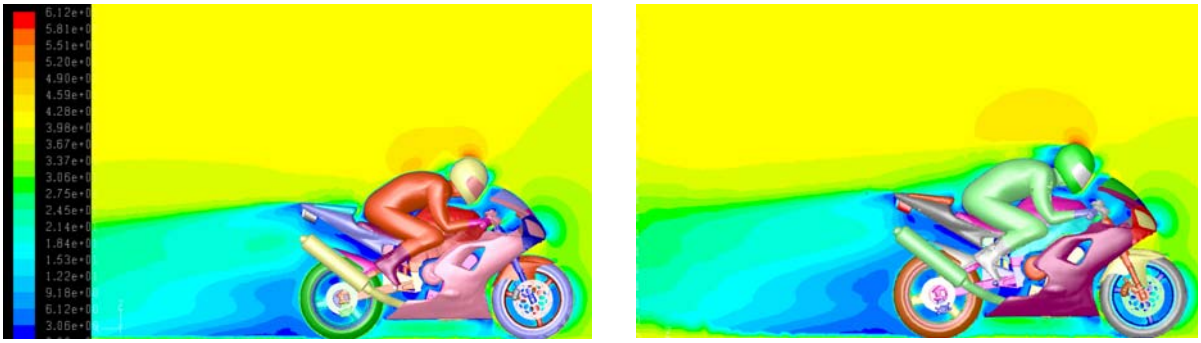

Figure 19: Velocity contours for fine tetra mesh (left) and coarse tetra mesh plus layers (left).

Figure 20 shows the y^+ contours on the surface for the tetra coarse and the tetra coarse plus layers. It is clear the the model with the layers is more suitable for the application of the non equilibrium wall functions and the boundary layer flow is better resolved.

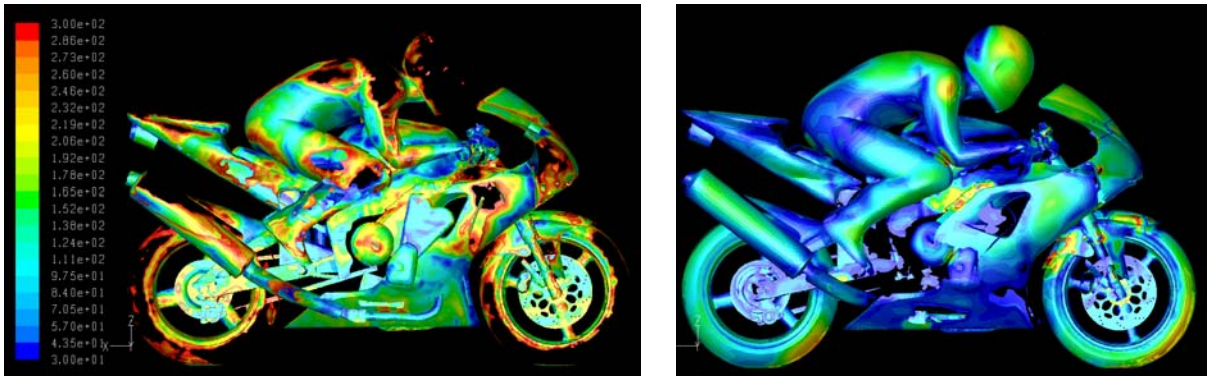

Figure 20: y^+ contours in the range of 30 to 300 for the coarse tetra mesh (left) and the coarse tetra mesh plus layers (right).

Figure 21 displays the velocity vectors at the centre plane and clearly shows that the plain tetra mesh cannot predict the separation that the tetra plus layers model can, near the top of the helmet. The fine tetra mesh did not either predict the separation, and gave exactly the same results as the coarse tetra.

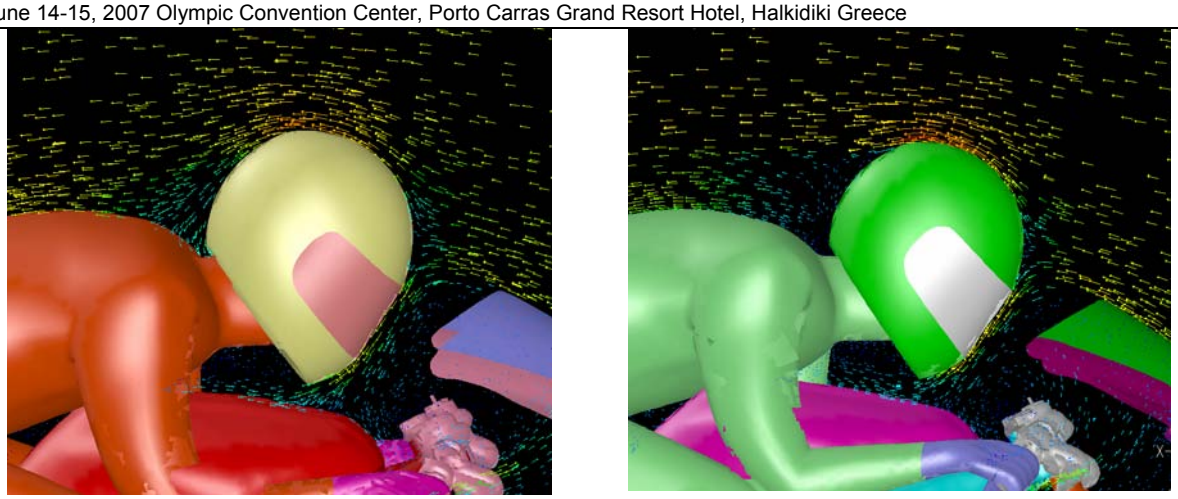

Figure 21: Velocity vectors for coarse tetra mesh (left) and
coarse tetra mesh plus layers (right).
The model with layers predicts the separation near the top of the helmet

Figure 22 shows also how the tetra plus layers model accurately predicts the skin friction on the surface and the abrupt drop to zero at the separation area.
Finally, Figure 23 shows the different streamline pattern without and with the predicted separation.

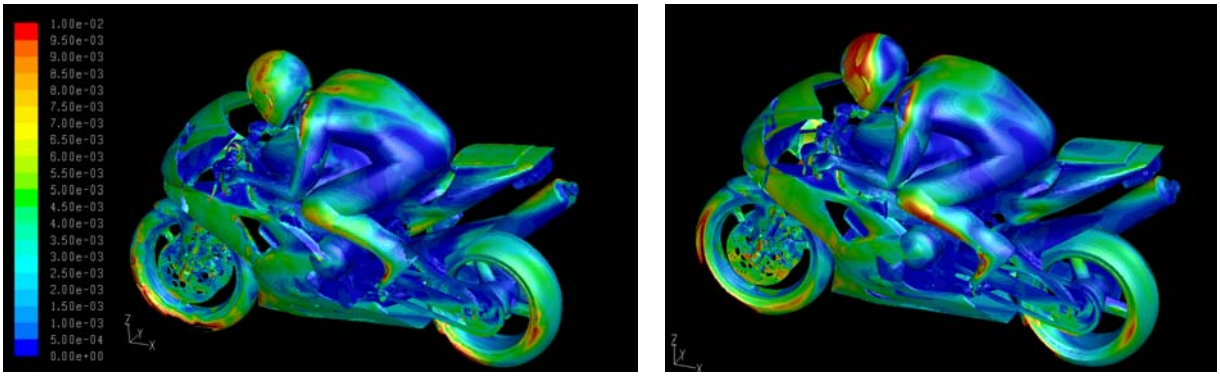

Figure 22: Skin friction coefficient contours for coarse tetra mesh (left) and
coarse tetra plus layers mesh (right)

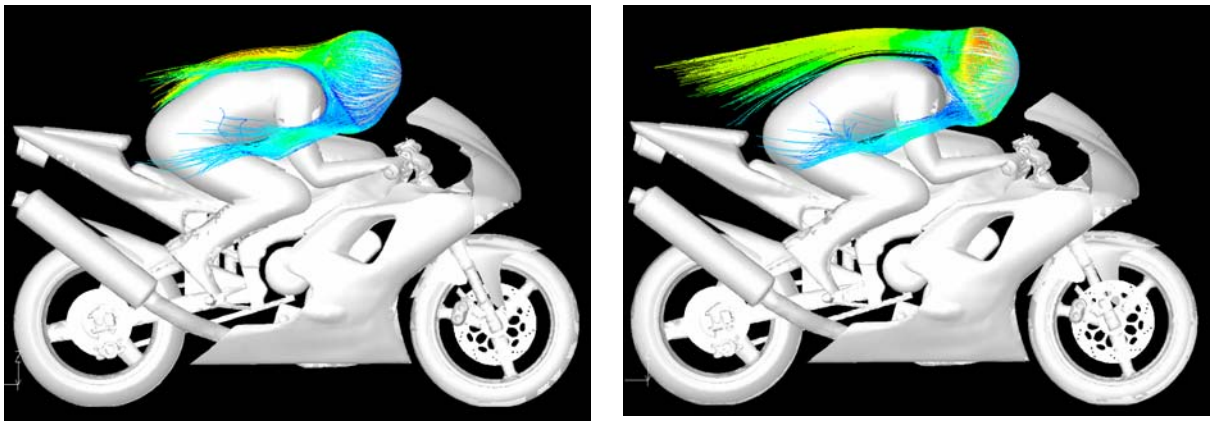

Figure 23: Streamlines released from helmet for coarse tetra mesh (left) and
coarse tetra plus layers mesh (right)

Still even with this discrepancy in the flow resolution, the resulting drag coefficient is very similar for both cases, as most of the drag comes from the main wake.

3.5 COMPARISON OF RESULTS BETWEEN ORIGINAL AND MORPHED MODEL

The last simulations were performed on the tetra coarse mesh for the original and the morphed geometry. Table 3 shows the predicted drag and lift coefficients for the two models. The sensitivity of the simulation to this geometrical change is evident as the drag was increased by 7% and the lift coefficient was reduced by 46 %.

	C_D pressure	C_D viscous	C_D total	C_L total
tetra original (3.1 million)	0.435	0.022	0.457	0.098
tetra morphed (3.1 million)	0.467	0.024	0.491	0.053

Table 3: Simulation results for original and morphed models of tetra coarse mesh

Figure 24 shows the pressure coefficient distribution, where it is evident that in the morphed model a lot of the frontal high pressure area was moved from the rider's helmet to the front fairing of the motorcycle. Figure 25 shows the streamlines near the centre plane.

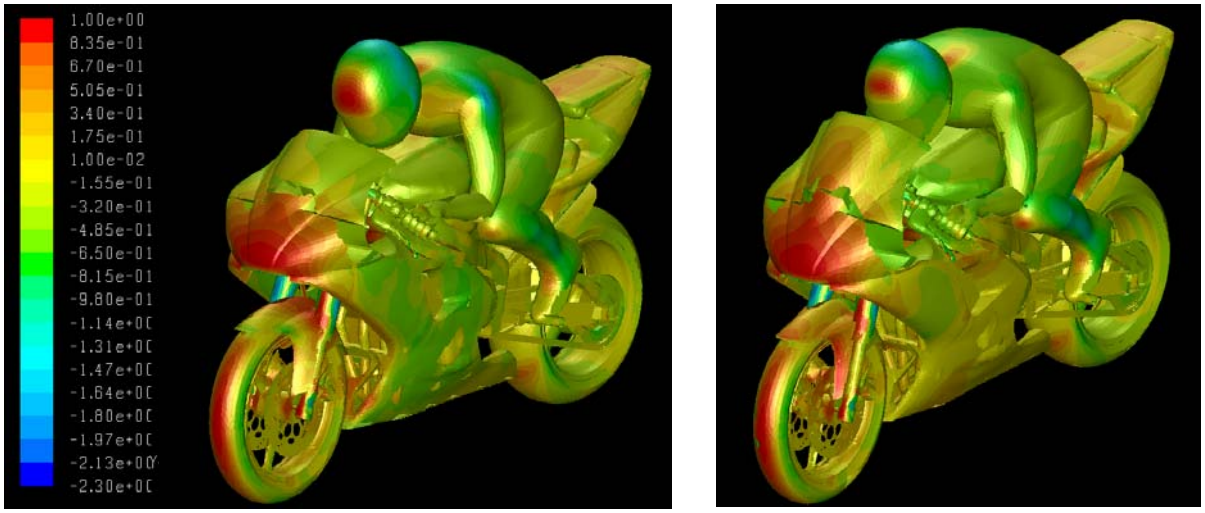

Figure 24: Pressure coefficient contours for original model (left) and morphed model (right) for the same coarse tetra mesh

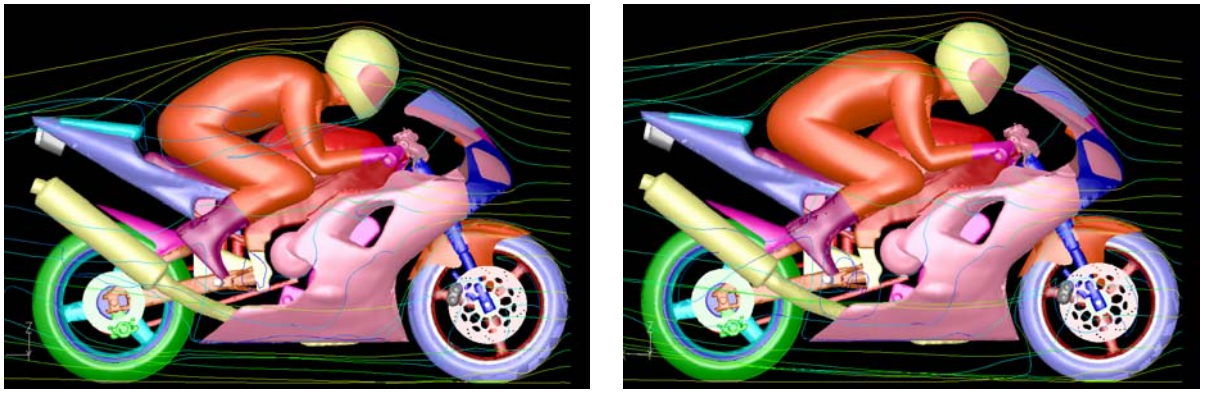

Figure 25: Streamlines for original model (left) and morphed model (right) for the same coarse tetra mesh

3.6 COMPARISON WITH LITERATURE RESULTS

A literature survey was made to collect some experimental results from similar motorcycles [6-8]. Table 4 gives a summary of these findings which are in good agreement with the CFD simulations in this work, bearing in mind all variations in motorcycle geometries and of course in rider characteristics. In particular, the findings of Meijaard [7] and Sharp [8], which are the most recent ones, are in very good agreement, taking into consideration the sensitivity of the results to the morphing of the front upper fairing.

4. CONCLUSIONS

ANSA performed successfully all the tasks involved in the complete and efficient preparation and modification of a high quality mesh with feature dependant surface mesh, boundary layer generation from complex geometries and user controlled volume mesh, with minimum effort. All meshes gave very similar results in drag and lift coefficient prediction, which correlate very well to relevant literature data, indicating the quality of all the models. Only the mesh with the layers was capable of predicting the separation around the rider helmet, showing the importance of the presence of the layers when accurate results are required. ANSA morphing was performed successfully and efficiently and demonstrated the sensitivity of the CFD simulation on model geometrical changes.

	A	C_D	$C_D \cdot A$	C_L	$C_L \cdot A$	Reference
Kawasaki ZX-10 	0.70	0.50	0.35	-	-	Hucho [6]
Kawasaki KR 250 	0.45	0.49	0.22	0.11	0.05	Hucho [6]
Suzuki GSXR-1100 	0.71	0.52	0.37	-	-	Hucho [6]
YAMAHA TZR-250 	-	-	0.30	-	0.01	Hucho [6]
YAMAHA FZR-1000 	0.65	0.52	0.34	-	-	Hucho [6]
Aprilia RSV 1000 	-	-	0.27	-	-	Meijaard [7]
TRIUMPH	0.65	0.48	0.31	0.078	0.051	Sharp [8]
CFD model 	0.645	0.457	0.295	0.098	0.063	this work
Morphed CFD model 	0.645	0.491	0.317	0.053	0.034	this work

Table 4: Comparison of literature data (frontal area, drag and lift coefficients) and simulation results (*although not depicted in the images, values include rider lying forward*).

REFERENCES

(1) M. Ehlen, "ANSA as a pre-processor for CFD simulations with Fluent", 1st International ANSA and META Congress, June 2005

(2) S. di Piazza, D. Nanni, R. Rossi, "Numerical Multiscale Analysis of the Ducatti 999 Motorbike Heat Exchangers", Proceedings of the 2nd EACC, Fluent Inc., 2005

(3) R. Lewis, M. Cross, "Optimization using CFD and Mesh Deformation", Proceedings of the 2nd EACC, Fluent Inc., 2005

(4) M. Lanfrit, "Best Practice Guidelines for Handling Automotive External Aerodynamics with FLUENT", Version 1.2, http://www.fluentusers.com, 2005

(5) Z. Yang, J. Bozeman, F. Shen, D. Turner, S. Vemuri, "CFRM Concept for Vehicle Thermal System", SAE 2002-01-1207, 2002

(6) Wolf-Heinrich Hucho, "Aerodynamics of Road Vehicle" Fourth Edition, SAE international, 1998

(7) J.P. Meijaard, A. A. Popov, "Influences of Aerodynamic Drag, the Suspension System and Rider's Body Position on Instabilities in a Modern Motorcycle" Vehicle System Dynamics, Vol. 44. Supplement pp690-697, 2006

(8) R. Sharp, S. Evangelou, D. J. N. Limebeer, " Advances in the Modelling of Motorcycle Dynamics", Multibody System Dynamics, Vol. 12, pp251-283, 2004